Journal of Materials Chemistry C

Ambipolar transistors based on chloro-substituted tetraphenylpentacene

Journal:	*Journal of Materials Chemistry C*
Manuscript ID	TC-ART-12-2018-006603.R1
Article Type:	Paper
Date Submitted by the Author:	01-Feb-2019
Complete List of Authors:	Sato, Ryonosuke; Tokyo Institute of Technology, Department of Organic and Polymeric Materials Eda, Shohei; Kwansei Gakuin University - Kobe Sanda Campus; Institute of Physical and Chemical Research Sugiyama, Haruki; Tokyo Institute of Technology; Keio University - Hiyoshi Campus Uekusa, Hidehiro; Tokyo Institute of Technology, Hamura, Toshiyuki; Kwansei Gakuin University, Department of chemistry Mori, Takehiko; Tokyo Institute of Technology , Department of Organic and Polymeric Materials

Journal Name

RSCPublishing

ARTICLE

Ambipolar transistors based on chloro-substituted tetraphenylpentacene†

Cite this: DOI: 10.1039/x0xx00000x

Ryonosuke Sato,[*a] Shohei Eda,[bc] Haruki Sugiyama,[de] Hidehiro Uekusa,[d] Toshiyuki Hamura,[*c] and Takehiko Mori[*a]

Received 00th January 2012,
Accepted 00th January 2012

DOI: 10.1039/x0xx00000x

www.rsc.org/

Thin-film transistors of halogen-substituted tetraphenylpentacenes are investigated. These compounds exhibit mainly hole transport, but the chlorine compound shows considerably higher performance than the fluorine and bromine compounds. In addition, the chlorine compound shows ambipolar properties, though the hole mobility is by four times larger than the electron mobility. These compounds have basically the same crystal structures, but the remarkable halogen dependence is explained from the critical location of the LUMO levels as well as the intermolecular transfers, which sensitively changes depending on the stacking geometry. In particular, hole and electron transfers exhibit different periodicity depending on the slip distance along the molecular long axis, and this is related to the appearance of the electron transport properties.

Introduction

Transistors of rubrene have been extensively studied owing to the highest performance in single-crystal organic transistors.[1–5] Rubrene has a uniformly stacking structure,[6] and it is comparatively difficult to make the thin-film transistors. On the other hand, pentacene is a representative transistor material,[7,8] and the thin-film transistors have been investigated for a long time. A variety of the related compounds have been investigated as transistor materials,[9–11] among which the tetramethyl and dibromo derivatives have been reported to show hole-transporting properties with the mobility of 0.2-0.3 $cm^2\ V^{-1}\ s^{-1}$,[12,13] and perfluoropentacene is known to show electron-transporting properties.[14] In this connection, tetraphenylpentacene is interesting (*X* = H in Scheme 1), which has been reported to show the hole mobility of $10^{-3}\ cm^2\ V^{-1}\ s^{-1}$ in the thin-film transistors.[15]

Usually pentacene shows only hole transport, and electron transport is observed only when calcium is used as the electrode material.[16] However, ambipolar transport is observed using Ag electrodes on poly(methyl methacrylate) (PMMA),[17] and Ag/Al electrodes on tetratetracontane (TTC).[18] TTC is an excellent passivation layer even when Au electrode is used, which enables the observation of ambipolar transistor properties in copper phthalocyanine,[18–20] indigos,[21–24] quinoidal oligothiophene,[25] semiquinones,[26] diketopyrrolopyrroles,[27,28] and isoindigos.[29,30]

We have recently developed a versatile synthetic route to prepare substituted acenes using cycloaddition reactions.[31–33] Using this route, we can directly obtain acenes where the terminal hydrogens are substituted by halogens. Carrier polarity is sensitive to terminal halogens because of the induced polarization.[9] In the present paper, thin-film transistors of halogen-substituted tetraphenylpentacenes (**4*X*4Ph**, where *X* = F, Cl, and Br in Scheme 1) are investigated.

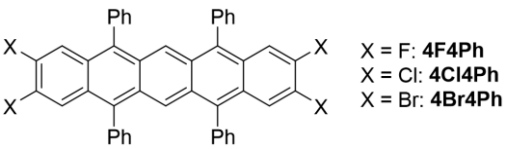

Scheme 1. Molecular structures of **4*X*4Ph**.

Experimental

Synthesis

The halogen-substituted tetraphenylpentacenes **4*X*4Ph** were prepared in two ways by using dibromodiphenylisobenzofuran **2c** as a synthetic building block (Scheme 2). Thus, the *one-pot* successive [4+2] cycloadditions of dihaloarynes and isobenzofurans efficiently gave diepoxypentacenes **4X4Ph_epoxy** (X = F, Cl),[31] which were converted to

pentacenes **4F4Ph** and **4Cl4Ph** by reductive aromatization (Scheme 2a). On the other hand, due to the poor site-selectivity in the bromine–lithium exchange of the tetrabromoepoxyanthracene **3c** for generation of aryne, pentacene **4Br4Ph** was alternatively prepared in four-steps including double Diels–Alder reactions of isobenzofuran **2c** and 1,4-benzoquinone as a key reaction (Scheme 2b).

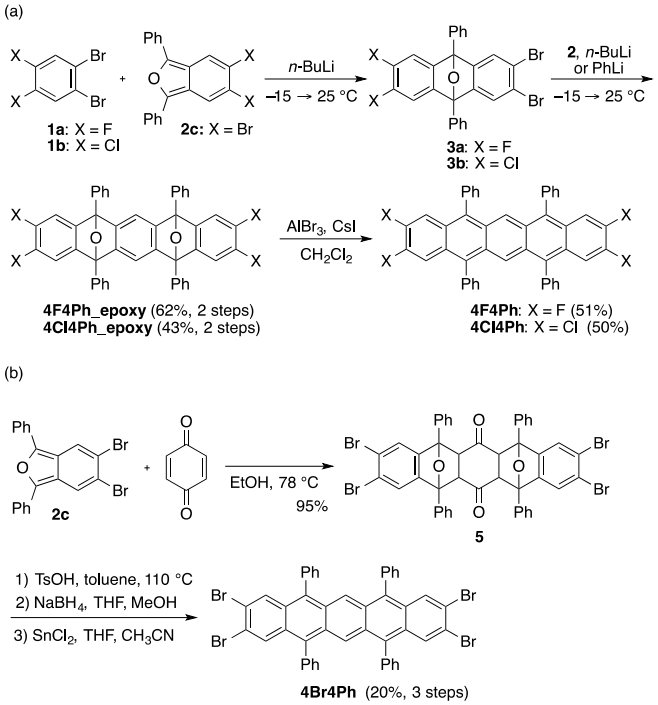

Scheme 2. Syntheses of pentacenes **4X4Ph**.

Device fabrication

Thin-film transistors were fabricated onto an n-doped Si substrate with a thermally grown SiO_2 dielectric layer (300 nm, C = 11.5 nF cm^{-2}). The passivation layer tetratetracontane ($C_{44}H_{90}$, TTC, e = 2.5) with a thickness of 20 nm was evaporated under a vacuum of 10^{-4} Pa on the substrates,[19,20] where the calculated overall capacitance of the gate dielectrics was 10.4 nF/cm^2.[34] Then **4*X*4Ph** with a thickness of 50 nm was evaporated. The top-contact electrodes were patterned by Au thermal deposition through a metal mask; the channel length (L) and width (W) were 100 μm and 1000 μm, respectively. The measurements were conducted under the vacuum of 10^{-3} Pa by using a Keithley 4200 semiconductor parameter analyzer. The mobilities were estimated from the saturated-region transfer characteristics.

Results and discussion

Energy levels

The highest occupied molecular orbital (HOMO) levels and the lowest unoccupied molecular orbital (LUMO) levels together with the energy gaps are summarized in Table 1. The HOMO levels are estimated from the oxidation potentials of the cyclic voltammograms, and the energy gaps are obtained from the absorption edges (Figs. S2 and S3, ESI†). Accordingly, the LUMO levels are evaluated by adding the energy gaps to the HOMO levels. Energy levels of the halogen substituted compounds are lower than those of the unsubstituted pentacene (HOMO/LUMO = –5.0/–3.2 eV)[35] and the tetraphenylpentacene (X = H, –4.95/–3.07 eV).[36] In general, a F substituted compound is a stronger acceptor than the corresponding Cl and Br compounds. In the present series, however, the LUMO levels indicate that **4F4Ph** is a weaker acceptor than **4Cl4Ph** and **4Br4Ph**. The HOMO levels are not largely different, but the optical gaps of **4Cl4Ph** and **4Br4Ph** are obviously smaller than that of **4F4Ph**. The difference of the LUMO levels may be attributed to the spread of the molecular orbitals to the halogen atoms. It has been reported that hole-transporting properties appear when the HOMO level is higher than –5.6 eV, whereas electron-transporting properties appear when the LUMO level is lower than –3.2 eV.[37] The HOMO levels of these compounds are much within the threshold. The LUMO levels of **4Cl4Ph** and **4Br4Ph** are certainly within the electron transporting limit, but **4F4Ph** and **4H4Ph** are critically out of the limit. Therefore, the energy levels indicate hole dominant ambipolar transport, but the electron transport may potentially depend on the substituents.

Table 1. Energy levels and gaps of **4*X*4Ph**.

X	E_{HOMO} (eV)	E_{LUMO} (eV)	Absorption edge (nm)	E_g (eV)
H	–5.01	–3.07	638	1.94
F	–5.17	–3.18	622	1.99
Cl	–5.19	–3.29	651	1.90
Br	–5.20	–3.31	656	1.89

Transistor properties

Thin-film transistors with bottom-gate top-contact geometry were fabricated onto a TTC-treated SiO_2 layer, where **4*X*4Ph** was thermally evaporated. The transfer and output characteristics are shown in Fig. 1. From these characteristics, the transistor parameters are extracted as summarized in Table 2. All compounds show hole transport, whereas only **4Cl4Ph** shows ambipolar transport. The hole mobility of **4Cl4Ph** (0.016 cm^2 V^{-1} s^{-1}) is much higher than those of **4F4Ph** and **4Br4Ph**. This mobility is also much larger than the reported value (10^{-3} cm^2 V^{-1} s^{-1}) of **4H4Ph**.[15] The hole mobility of **4Cl4Ph** is by four times larger than the electron mobility. The electron threshold voltage is also considerably larger than the hole threshold voltage. Then, the hole transport is obviously dominant. This is also evident

Table 2. Transistor properties of **4*X*4Ph**.

Compounds		μ_{ave} [μ_{max}] (cm^2 V^{-1} s^{-1})	V_{th} (V)	I_{on}/I_{off}
4F4Ph	p	4.4×10^{-5} [6.0×10^{-5}]	–9	5×10^2
4Cl4Ph	p	0.013 [0.016]	–5	3×10^3
	n	3.3×10^{-3} [6.4×10^{-3}]	58	2×10^5
4Br4Ph	p	2.3×10^{-4} [2.9×10^{-4}]	3	3×10^4

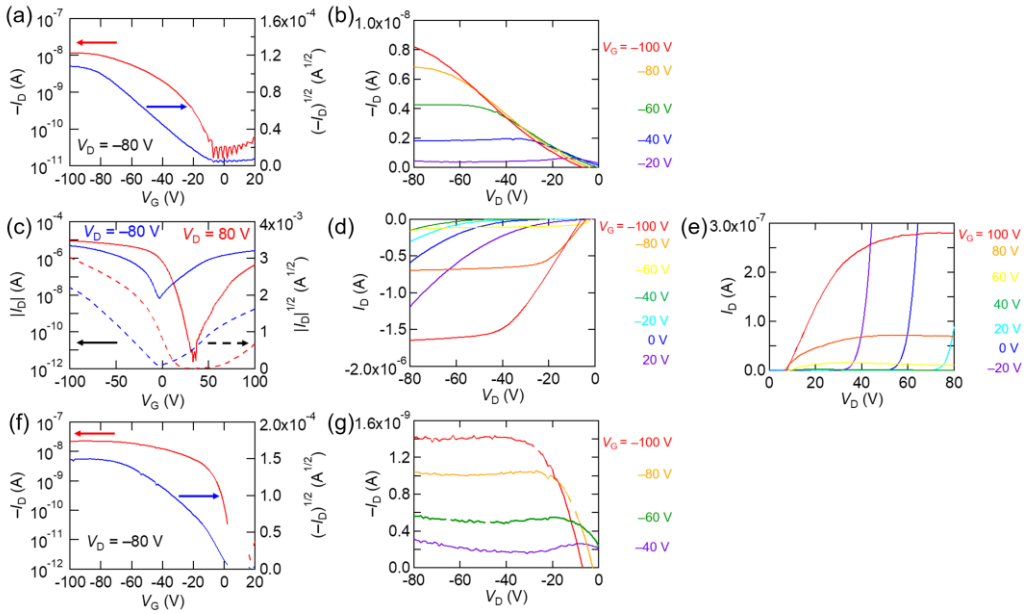

Figure 1. (a) Transfer and (b) output characteristics of **4F4Ph**. (c) Transfer and (d and e) output characteristics of **4Cl4Ph**. (f) Transfer and (g) output characteristics of **4Br4Ph**.

in the output characteristics (Fig. 1d), where the inverse current due to the electron transport is comparatively small, whereas large inverse current due to the hole transport is observed even from a positive V_D = 20 V in Fig. 1e.

Crystal structures

The crystal data are listed in Table 3. These compounds are approximately isostructural, where the stacking structure has close resemblance to rubrene (Fig. 2).[6] Torsion angles of phenyl groups from the pentacene skeleton are 58.7-66.0° in **4F4Ph**, 62.0-72.9° in **4Cl4Ph**, and 67.6-86.7° in **4Br4Ph**, which tend to be smaller than 80.8° in rubrene (Table S1, ESI†).[6] In addition, the rubrene molecule is located on an inversion center, whereas the present molecules are located on a general position. In contrast to rubrene with uniform stacks, the present compounds have dimerized stacks similar to tetrafluorotetraphenylanthracene.[38] Here, *c*1 with the distance between the molecular centers R ~ 4.9 Å makes a dimer (Table 4), and *c*2 (R > 8.7 Å) corresponds to the interdimer interaction.

In order to analyze the intermolecular interactions, the transfer integrals t are calculated for HOMO (t_h) and LUMO (t_e) as listed in Table 4.[39] Interstack transfers are negligibly small, and not shown in Table 4. The transfers are estimated from the HOMO and LUMO overlaps. As another method, the transfers are evaluated from the level splitting of the diads. Although the signs of transfers are not determined in the later method, both of these two calculation methods show the same tendency: $|t_h| > |t_e|$, indicating hole dominant transport. The comparatively high LUMO levels are the principal reason of the hole dominant transport, but the small electron bandwidth is also responsible.

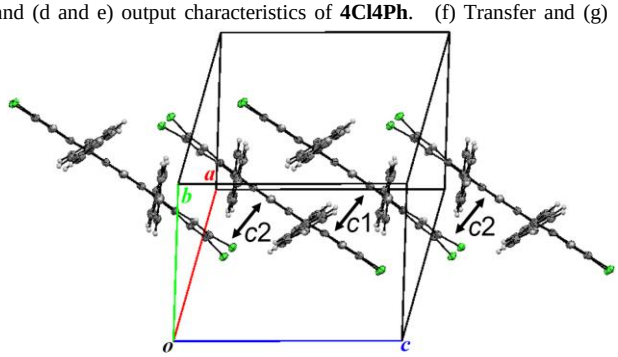

Figure 2. Crystal structure of **4Cl4Ph**.

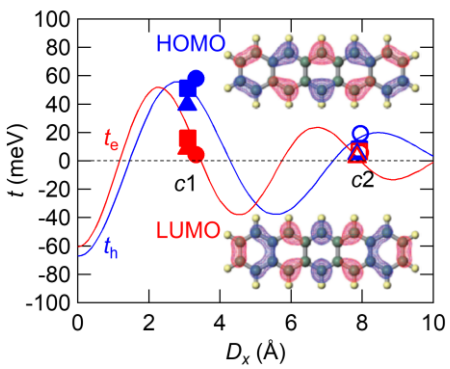

Figure 3. Intermolecular transfers as a function D_x at D_y = 0 Å and D_z = 3.4 Å, together with HOMO and LUMO of pentacene.[40] Circles are for **4F4Ph**, squares for **4Cl4Ph**, and triangles for **4Br4Ph**.

The bandwidth is determined by *c*2, and the interdimer $|t_e|$ (*c*2) of **4Br4Ph** (1.9 meV) is particularly small; this may be related to the absence of electron transport in **4Br4Ph**. It is

Table 3. Crystallographic data of **4*X*4Ph** (*X* = F, Cl, and Br).

Crystal	**4F4Ph**	**4Cl4Ph**	**4Br4Ph**
Formula	$C_{46}H_{26}F_4$	$C_{46}H_{26}Cl_4$	$C_{46}H_{26}Br_4$
Formula weight	654.67	720.47	898.31
Crystal size (mm^3)	0.07 × 0.06 × 0.02	0.122 × 0.071 × 0.031	0.099 × 0.048 × 0.033
μ (mm^{-1})	0.789	0.388	5.826
Crystal system	Triclinic	Triclinic	Triclinic
Space group	*P*–1	*P*–1	*P*–1
Z	2	2	2
a (Å)	10.0390(2)	10.3770(13)	10.3811(3)
b (Å)	13.0700(2)	12.874(2)	13.2135(4)
c (Å)	13.4090(2)	13.3509(17)	13.8306(4)
α (deg)	112.658(1)	86.033(6)	81.924(2)
β (deg)	103.943(1)	77.911(4)	77.158(2)
γ (deg)	92.256(1)	74.579(5)	72.986(2)
V ($Å^3$)	1558.15(5)	1681.1(4)	1762.94(9)
ρ (g cm^{-3})	1.395	1.423	1.692
Total reflns.	18385	16286	20752
Unique reflns. (R_{int})	5593 (0.0399)	7546 (0.0693)	6332 (0.1139)
R_1 ($F^2 > 2\sigma(F^2)$)	0.0677	0.0694	0.0685
wR_2 (All reflections)	0.2312	0.2303	0.1983
GOF	0.968	1.029	1.013
Temperature (K)	173(2)	93(2)	123(2)

characteristic of **4Cl4Ph** that the intradimer $|t_e|$ (*c*1) is larger than those of **4F4Ph** and **4Br4Ph**. In particular, the intradimer $|t_e|$ (*c*1) of **4F4Ph** is even smaller than *c*2, and the bandwidth is limited by *c*1. This is a reason that the electron transport in **4F4Ph** is hampered rather than naively expected from the geometry.

Since transfer integrals are sensitive to the geometry of the diads,[40] slip distances along the molecular long axis (D_x) and along the molecular short axis (D_y) are evaluated as well as the interplanar distances (D_z) (Table 4). It is reasonable that *c*2 interaction with large D_x ~ 7.9 Å affords a smaller transfer than the *c*1 interaction with small D_x ~ 3.1 Å. Since the HOMO and LUMO have nodes on each benzene ring,[40] the transfer is a periodical function of D_x (Fig. 3). The previous calculation indicates that the HOMO transfer has peaks at D_x = 0, 2.8, 5.6, and 8.5 Å, in which 2.8 Å corresponds to the size of a benzene ring.[40] The *c*1 and *c*2 overlaps are not far from the second and fourth peaks, leading to a comparatively large $|t_h|$. The LUMO transfer periodicity is slightly smaller than this, which makes peaks at D_x = 0, 2.3, 4.5, 6.7, and 8.9 Å. This is because the HOMO spreads to the outer rings, but the LUMO spreads to the inner rings (Fig. 3).[40] Accordingly, the LUMO transfer has nodes at D_x = 1.2, 3.5, 5.8, and 8.0 Å. The actual D_x values of the present crystals are not definitely on the LUMO peaks, and particularly that of *c*2 (D_x ~ 7.9 Å) is close to the node. D_x values of **4Cl4Ph** and **4Br4Ph** for *c*1 are 3.1 Å, but that of **4F4Ph** *c*1 is 3.3 Å (Table 4), which is around the node of the LUMO transfer (D_x = 3.5 Å).[40] This is the reason of significantly small *c*1 in **4F4Ph**. Similar D_x sensitivity has been recently reported in halogenated tetraazapentacenes as well.[41]

Table 4. Intermolecular transfer integrals and slip distances in **4*X*4Ph**.

Compounds		Transfer integrals (meV)[a]		Slip distances (Å)[b]			
		t_h	t_e	D_x	D_y	D_z	*R*
4F4Ph	*c*1	–58.1 (48.2)	4.4 (0.8)	3.32	0.05	3.66	4.94
	*c*2	–19.4 (16.8)	–5.9 (9.0)	7.95	0.46	3.60	8.74
4Cl4Ph	*c*1	–51.1 (43.2)	15.9 (9.4)	3.09	0.32	3.68	4.82
	*c*2	–8.2 (8.8)	–6.6 (8.4)	7.92	1.11	3.74	8.82
4Br4Ph	*c*1	–39.6 (34.6)	8.8 (5.2)	3.08	0.43	3.85	4.96
	*c*2	4.8 (3.2)	–1.9 (2.9)	7.85	2.09	4.23	9.16

[a] From orbital overlaps. Values in the parentheses are from level splittings.
[b] Slip distances in a diad from the definitions indicated below. *R* is the distance between the molecular centers.

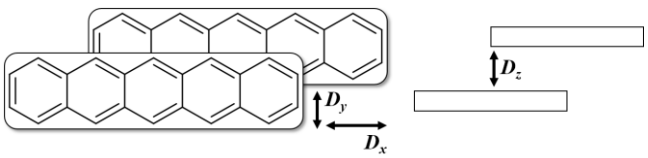

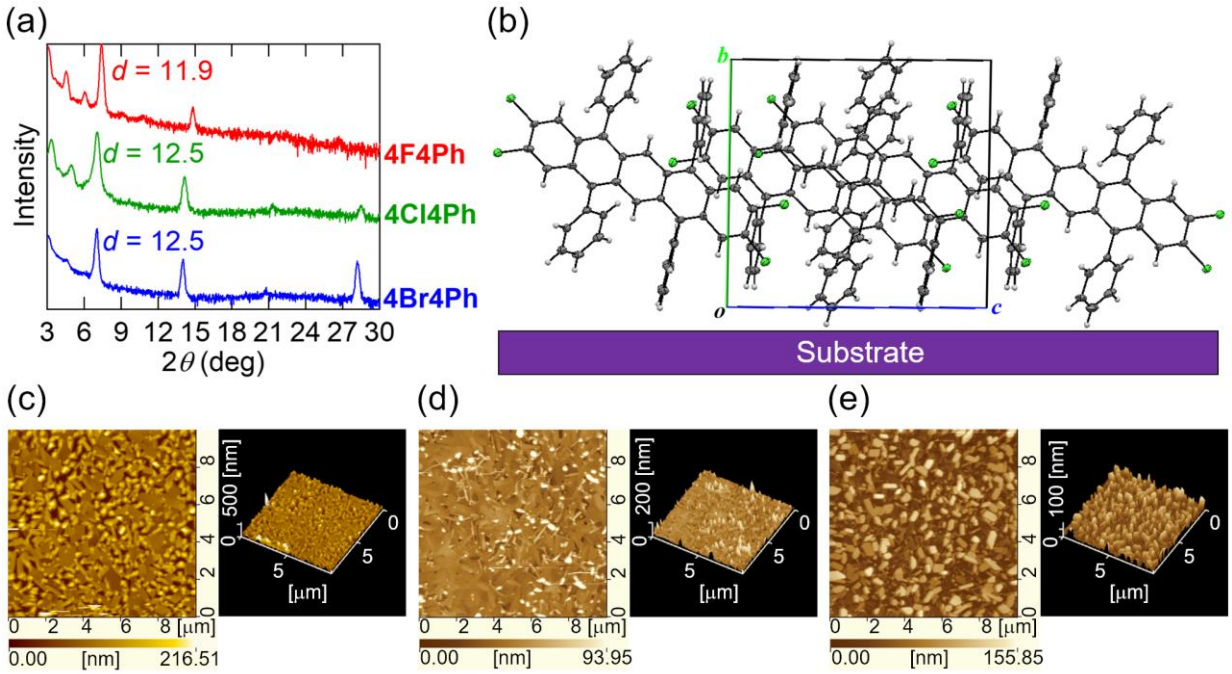

Figure 4. Thin-film properties of **4*X*4Ph**. (a) XRD patterns and (b) molecular orientation in the thin-film **4Cl4Ph**. AFM images of (c) **4F4Ph**, (d) **4Cl4Ph**, and (e) **4Br4Ph**.

In addition, we could not neglect the influence of the nonzero D_y (Figs. S4-S9, ESI†). The *c*2 interaction of **4Br4Ph** has exceptionally large D_y = 2.09 Å and D_z = 4.23 Å, which is related to the poor transistor performance. Accordingly, the absence of electron transport in **4F4Ph** is probably related to the small *c*1 value for electron together with the high LUMO level, whereas the difference of **4Cl4Ph** and **4Br4Ph** is derived from the magnitude of the *c*2 values.

Thin-film properties

X-ray diffraction (XRD) patterns, and atomic force microscopy (AFM) images of the thin films deposited on the tetratetracontane (TTC)-modified Si/SiO_2 substrates were observed. As shown in Fig. 4a, the XRD patterns show diffraction peaks around 2θ = 7.1~7.4°. The *d*-spacings, 11.9~12.5 Å, correspond to $b \sin\alpha \sin\gamma$ of the crystal lattice, indicating that the crystallographic *ac* plane is aligned parallel to the substrate (Fig. 4b). Not only the (010) peaks but also the (020) peaks are observed in the three films, and the (040) peaks are observed in the **4Cl4Ph** and **4Br4Ph** films. The pentacene core has the side-on arrangement rather than the end-on arrangement. Then, the terminal halogen atoms do not contribute to the polarization at the gate interface. This is a reason that charge polarity does not depend on the halogen electron negativity. The molecular planes are tilted by 65.4° (**4F4Ph**), 70.2° (**4Cl4Ph**), and 74.6° (**4Br4Ph**) with respect to the substrates.

The **4Br4Ph** molecules are standing most close to the perpendicular direction to the substrate. It has been generally known that the mobility attains a maximum at the perpendicular molecular arrangement.[24] This may be the reason that the mobility of **4Br4Ph** is five times larger than that of **4F4Ph**.

Atomic force microscopy (AFM) images of the thin films are shown in Figs. 4c-e. Grains of three films are in the same size of about 1 μm. However, in the **4F4Ph** and **4Br4Ph** films, rod-like microcrystals cover the substrate, but in the **4Cl4Ph** film, plate-like microcrystals densely cover the substrate. The **4F4Ph** and **4Br4Ph** films show relatively sparse coverage in comparison with the **4Cl4Ph** film. The **4F4Ph** film shows larger roughness than the **4Cl4Ph** and **4Br4Ph** films, and this may be related to the absence of the (040) XRD peak in the **4F4Ph** film. The thin-film quality is to some extent responsible for the largely different mobilities of these materials.

Conclusions

Thin-film transistors of **4*X*4Ph** show mainly hole transport. **4Cl4Ph** exhibits higher performance than **4F4Ph** and **4Br4Ph**. In addition, **4Cl4Ph** shows electron transport as well. These compounds have basically the same crystal structures, but the remarkable halogen dependence as well as the hole dominant transport is explained from the critical location of the LUMO levels as well as the intermolecular transfers which sensitively changes depending on the stacking geometry. In particular, the periodicity of the LUMO transfer is different from that of the HOMO transfer, and sensitively influences the appearance of electron transport.

Acknowledgments

We thank Dr. H. Kojima (Nara Institute of Science and Technology) for the results in Fig. 3, which are taken from Ref. 40. This work was partly supported by ACT-C Grant Number JPMJCR12YY and JPMJCR12ZB from JST, Japan, a Grant-in Aid for Scientific Research (No. 16K13974, 18H02044, and 15H05840) from the Ministry of Education, Culture, Sports, Science, and Technology of Japan, and Takahashi Industrial and Economic Research Foundation. The authors are grateful to the Tokyo Institute of Technology Center for Advanced Materials Analysis for XRD measurement and Prof. Kakimoto for AFM measurements.

Notes and references

[a] Department of Materials Science and Engineering, Tokyo Institute of Technology, O-okayama, Meguro-ku, Tokyo 152-8552, Japan. *E-mail: sato.r.ah@m.titech.ac.jp, mori.t.ae@m.titech.ac.jp
[b] Department of Applied Chemistry and Environment, Kwansai Gakuin University, 2-1 Gakuen, Sanda, Hyogo 669-1337, Japan. *E-mail: thamura@kwansei.ac.jp
[c] Present address: RIKEN, 2-1, Hirosawa, Wako, Saitama 351-0198, Japan.
[d] Department of Chemistry, Tokyo Institute of Technology, O-okayama, Meguro-ku, Tokyo 152-8551, Japan.
[e] Present address: Research and Education Center for Natural Sciences, Keio University, 4-1-1 Hiyoshi, Kohoku-ku, Yokohama, Kanagawa 223-8521, Japan.

† Electronic supporting information (ESI) available: Additional information for preparative details, structure analysis, and transfer integrals. CCDC 1887275-1887277.

1 V. Podzorov, V. M. Pudalov and M. E. Gershenson, *Appl. Phys. Lett.*, 2003, **82**, 1739.
2 V. C. Sundar, J. Zaumseil, V. Podzorov, E. Menard, R. L. Willett, T. Someya, M. E. Gershenson and J. A. Rogers, *Science*, 2004, **303**, 1644.
3 V. Podzorov, E. Menard, A. Borissov, V. Kiryukhin, J. A. Rogers and M. E. Gershenson, *Phys. Rev. Lett.*, 2004, **93**, 086602.
4 R. W. I. de Boer, M. E. Gershenson, A. F. Morpurgo and V. Podzorov, *Phys. status solidi*, 2004, **201**, 1302.
5 J. Takeya, M. Yamagishi, Y. Tominari, R. Hirahara, Y. Nakazawa, T. Nishikawa, T. Kawase, T. Shimoda and S. Ogawa, *Appl. Phys. Lett.*, 2007, **90**, 102120.
6 O. D. Jurchescu, A. Meetsma and T. T. M. Palstra, *Acta Crystallogr. Sect. B Struct. Sci.*, 2006, **62**, 330.
7 C. D. Dimitrakopoulos and P. R. L. Malenfant, *Adv. Mater.*, 2002, **14**, 99.
8 H. Klauk, M. Halik, U. Zschieschang, G. Schmid, W. Radlik and W. Weber, *J. Appl. Phys.*, 2002, **92**, 5259.
9 A. R. Murphy and J. M. J. Fréchet, *Chem. Rev.*, 2007, **107**, 1066.
10 J. E. Anthony, *Angew. Chemie Int. Ed.*, 2008, **47**, 452.
11 K. Takimiya, S. Shinamura, I. Osaka and E. Miyazaki, *Adv. Mater.*, 2011, **23**, 4347.
12 H. Meng, M. Bendikov, G. Mitchell, R. Helgeson, F. Wudl, Z. Bao, T. Siegrist, C. Kloc and C.-H. Chen, *Adv. Mater.*, 2003, **15**, 1090.
13 T. Okamoto, M. L. Senatore, M.-M. Ling, A. B. Mallik, M. L. Tang and Z. Bao, *Adv. Mater.*, 2007, **19**, 3381.
14 Y. Sakamoto, T. Suzuki, M. Kobayashi, Y. Gao, Y. Fukai, Y. Inoue, F. Sato and S. Tokito, *J. Am. Chem. Soc.*, 2004, **126**, 8138.
15 Q. Miao, X. Chi, S. Xiao, R. Zeis, M. Lefenfeld, T. Siegrist, M. L. Steigerwald and C. Nuckolls, *J. Am. Chem. Soc.*, 2006, **128**, 1340.
16 T. Yasuda, T. Goto, K. Fujita and T. Tsutsui, *Appl. Phys. Lett.*, 2004, **85**, 2098.
17 L.-Y. Chiu, H.-L. Cheng, H.-Y. Wang, W.-Y. Chou and F.-C. Tang, *J. Mater. Chem. C*, 2014, **2**, 1823.
18 A. Opitz, M. Horlet, M. Kiwull, J. Wagner, M. Kraus and W. Brütting, *Org. Electron.*, 2012, **13**, 1614.
19 M. Kraus, S. Richler, A. Opitz, W. Brütting, S. Haas, T. Hasegawa, A. Hinderhofer and F. Schreiber, *J. Appl. Phys.*, 2010, **107**, 094503.
20 M. Kraus, S. Haug, W. Brütting and A. Opitz, *Org. Electron.*, 2011, **12**, 731.
21 M. Irimia-Vladu, E. D. Głowacki, P. A. Troshin, G. Schwabegger, L. Leonat, D. K. Susarova, O. Krystal, M. Ullah, Y. Kanbur, M. A. Bodea, V. F. Razumov, H. Sitter, S. Bauer and N. S. Sariciftci, *Adv. Mater.*, 2012, **24**, 375.
22 E. D. Głowacki, G. Voss and N. S. Sariciftci, *Adv. Mater.*, 2013, **25**, 6783.
23 O. Pitayatanakul, T. Higashino, T. Kadoya, M. Tanaka, H. Kojima, M. Ashizawa, T. Kawamoto, H. Matsumoto, K. Ishikawa and T. Mori, *J. Mater. Chem. C*, 2014, **2**, 9311.
24 O. Pitayatanakul, K. Iijima, M. Ashizawa, T. Kawamoto, H. Matsumoto and T. Mori, *J. Mater. Chem. C*, 2015, **3**, 8612.
25 T. Higashino, J. Cho and T. Mori, *Appl. Phys. Express*, 2014, **7**, 121602.
26 T. Higashino, S. Kumeta, S. Tamura, Y. Ando, K. Ohmori, K. Suzuki and T. Mori, *J. Mater. Chem. C*, 2015, **3**, 1588.
27 E. D. Głowacki, H. Coskun, M. A. Blood-Forsythe, U. Monkowius, L. Leonat, M. Grzybowski, D. Gryko, M. S. White, A. Aspuru-Guzik and N. S. Sariciftci, *Org. Electron.*, 2014, **15**, 3521.
28 K. Iijima and T. Mori, *Chem. Lett.*, 2017, **46**, 357.
29 M. Ashizawa, N. Masuda, T. Higashino, T. Kadoya, T. Kawamoto, H. Matsumoto and T. Mori, *Org. Electron.*, 2016, **35**, 95.
30 D. Yoo, T. Hasegawa, M. Ashizawa, T. Kawamoto, H. Masunaga, T. Hikima, H. Matsumoto and T. Mori, *J. Mater. Chem. C*, 2017, **5**, 2509.
31 H. Haneda, S. Eda, M. Aratani and T. Hamura, *Org. Lett.*, 2014, **16**, 286.
32 S. Eda, F. Eguchi, H. Haneda and T. Hamura, *Chem. Commun.*, 2015, **51**, 5963.
33 S. Eda and T. Hamura, *Molecules*, 2015, **20**, 19449.
34 K.-J. Baeg, Y.-Y. Noh, J. Ghim, B. Lim and D.-Y. Kim, *Adv. Funct. Mater.*, 2008, **18**, 3678.
35 T. Yasuda, T. Goto, K. Fujita and T. Tsutsui, *Appl. Phys. Lett.*, 2004, **85**, 2098.
36 I. Kaur, W. Jia, R. P. Kopreski, S. Selvarasah, M. R. Dokmeci, C. Pramanik, N. E. McGruer and G. P. Miller, *J. Am. Chem. Soc.*, 2008, **130**, 16274.
37 M. L. Tang, A. D. Reichardt, P. Wei and Z. Bao, *J. Am. Chem. Soc.*, 2009, **131**, 5264.
38 A. Izumoto, H. Kondo, T. Kochi and F. Kakiuchi, *Synlett*, 2017, **28**, 2609.
39 T. Mori, A. Kobayashi, Y. Sasaki, H. Kobayashi, G. Saito and H. Inokuchi, *Bull. Chem. Soc. Jpn.*, 1984, **57**, 627.
40 H. Kojima and T. Mori, *Bull. Chem. Soc. Jpn.*, 2011, **84**, 1049.
41 M. Chu, J.-X. Fan, S. Yang, D. Liu, C. F. Ng, H. Dong, A.-M. Ren and Q. Miao, *Adv. Mater.*, 2018, **30**, 1803467.

The table of contents entry

Title
Ambipolar transistors based on halogen-substituted tetraphenylpentacenes

Text (one sentence, of maximum 20 words, highlighting the novelty of the work)
Transistor properties of halogen-substituted tetraphenylpentacenes sensitively change depending on the slip distance along the molecular long axis.

Keywords
organic transistors, ambipolar transistors, transfer integral

Authors
Ryonosuke Sato, Shohei Eda, Haruki Sugiyama, Hidehiro Uekusa, Toshiyuki Hamura, and Takehiko Mori

ToC figure (maximum size 8 cm x 4 cm)